

Small-Order Shape Factors in In^{114} , P^{32} , and $\text{Y}^{90}\dagger$

R. T. NICHOLS,* R. E. MCADAMS, AND E. N. JENSEN

Institute for Atomic Research and Department of Physics, Iowa State University, Ames, Iowa

(Received November 7, 1960; revised manuscript received January 4, 1961)

The beta spectra of In^{114} , P^{32} , and Y^{90} have been studied closely in an intermediate-image beta-ray spectrometer and compared to theoretical predictions in terms of a linear shape factor of the form $(1+aW)$. The values obtained for a were $(+0.0036 \pm 0.0021)/mc^2$ for In^{114} , $(-0.0133 \pm 0.0011)/mc^2$ for P^{32} , and $(-0.0047 \pm 0.0008)/mc^2$ for Y^{90} , all for electron kinetic energies from about 200 keV up to near the maximum beta energies. Tests were made to give indications for spectrometer fidelity. Because of the linearity of the shape-factor plots and the similarity in energy range, the comparative results from In^{114} , P^{32} , and Y^{90} are taken as a definite indication that for at least two of these activities the shape factors have nonzero slopes, irrespective of questions of instrumental fidelity.

I. INTRODUCTION

THE form of the beta-decay interaction now seems to have been clarified¹ principally through experiments involving parity nonconservation. This removes the possibility of Fierz interference² and makes the theoretical beta-momentum distribution quite definite in many cases.

Although there persisted some degree of disagreement between the experimental results of beta spectroscopy and the Fermi theory until about 1943,³ the improved techniques of the past decade have given rise to a general agreement where linearity of Kurie (F-K) plots has been the test. In studies that have been made, having a precision of one percent or better per data point, there still remains some disagreement among the experimental results, thus indicating the frequent presence of instrumental distortions to at least this order of magnitude. In spite of the great success of the Fermi theory, a closer experimental check on beta spectra shapes still seems desirable.

Tests for spectrometer fidelity in general do not give sufficient information to constitute a proof of such. Unless the evidence is quite compelling, it may be more reasonable to accept the theory as a test for the experimental methods. However, as pointed out by Porter *et al.*,⁴ if one finds differences in beta spectra of similar energy range under the same experimental conditions, the reality of some deviation from the theory should be evident. The present work reports the results of a study of In^{114} , P^{32} , and Y^{90} under similar conditions. Some consideration is given to experimental indications of instrumental accuracy.

Recent investigations⁴⁻⁹ of these isotopes, employing

volatilized sources and thin ($\leq 200 \mu\text{g}/\text{cm}^2$) backings, have varied in results. P^{32} was included in each of these studies. The other results may best be compared in relation to the P^{32} values. The results from other isotopes which are common to two or more of these references should also be noted. The factor L_0 was not incorporated in the allowed shape factors of P^{32} in these works. It is almost constant for low Z isotopes, decreasing by 0.7% for P^{32} over the energy range from 250 to 1600 keV.

P^{32} and Y^{90} were examined by Pohm *et al.*⁵ in a thin-lens spectrometer and in an intermediate-image spectrometer. The Y^{90} shape-factor plots obtained from both instruments gave no indication of deviation from theory. The P^{32} shape factors changed about 1.5% over the interval from 300 keV to 1600 keV but in opposite directions for the two spectrometers. However, Henton and Carlson,⁶ using superior statistical methods on the same P^{32} data, found the shape factors from both spectrometers to have negative slopes, decreasing $(2.3 \pm 0.5)\%$ for the intermediate-image spectrometer and $(1.1 \pm 0.8)\%$ for the thin-lens spectrometer, over the energy interval from 300 keV to 1600 keV.

Porter, Wagner, and Freedman,⁴ using an iron-free double-lens spectrometer, found a decrease of about 3% in the P^{32} shape factor over the same energy range. Under the same conditions, Na^{24} , which has about the same energy, showed no deviation from theory.

Daniel⁷ obtained a linear shape-factor plot for P^{32} decreasing about 10% between 300 keV and 1600 keV and for Na^{24} found a decrease of $(3 \pm 1)\%$ from 200 keV to 1250 keV. Na^{22} results reported at the same time showed no deviation from theory. These data were also taken in a double-lens spectrometer.

Graham, Geiger, and Eastman⁸ investigated P^{32} with a double-lens spectrometer and found an excess of about

[†] Contribution No. 949. Work was performed in the Ames Laboratory of the U. S. Atomic Energy Commission.

* Present address: Gustavus Adolphus College, St. Peter, Minnesota.

¹ E. J. Konopinski, *Annual Review of Nuclear Science* (Annual Reviews, Inc., Palo Alto, California, 1959), Vol. 9, pp. 99.

² M. Z. Fierz, *Physik* **104**, 553 (1937).

³ C. S. Wu, *Revs. Modern Phys.* **22**, 386 (1950).

⁴ F. T. Porter, F. Wagner, Jr., and M. S. Freedman, *Phys. Rev.* **107**, 135 (1957).

⁵ A. V. Pohm, R. C. Waddell, and E. N. Jensen, *Phys. Rev.* **101**, 112, 2004 (1958).

1315 (1956). This article gives many references to earlier works on P^{32} and Y^{90} .

⁶ G. B. Henton and B. C. Carlson, U. S. Atomic Energy Commission Report ISC-1006 (Iowa State University) December, 1957 (unpublished); *Bull. Am. Phys. Soc.* **2**, 358 (1957).

⁷ H. Daniel, *Nuclear Phys.* **8**, 191 (1958).

⁸ R. L. Graham, J. S. Geiger, and T. A. Eastman, *Am. J. Phys.* **36**, 1084 (1958).

⁹ O. E. Johnson, R. G. Johnson, and L. M. Langer, *Phys. Rev.*

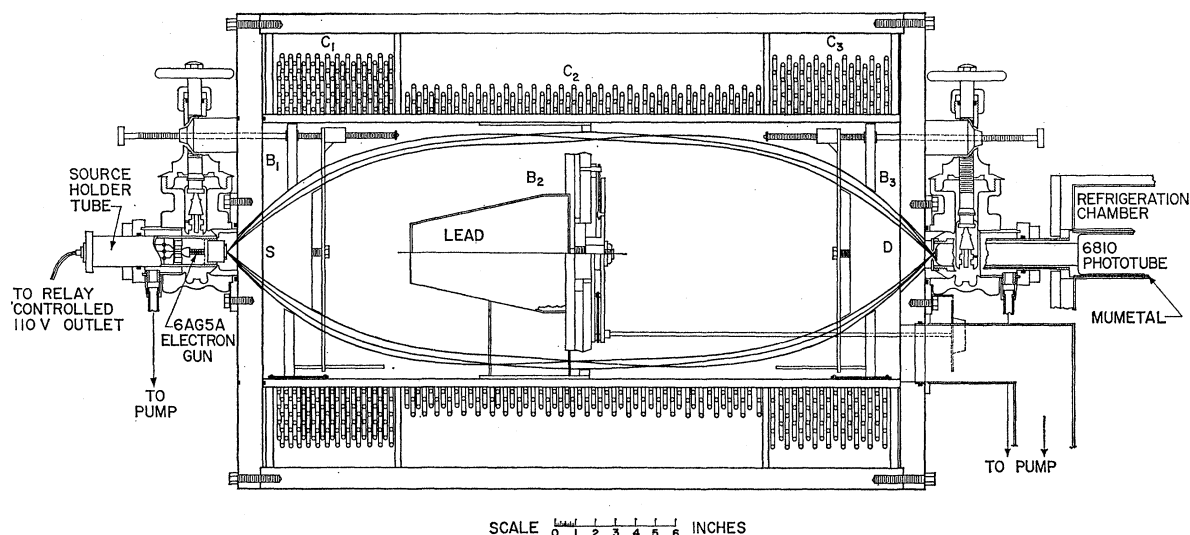


FIG. 1. Schematic diagram of spectrometer with modified endplates.

5% in the low-energy region of a shape-factor plot. They reported that no significant difference was seen in results from a volatilized source on $200\text{-}\mu\text{g}/\text{cm}^2$ backing and a liquid-deposited source on $800\text{-}\mu\text{g}/\text{cm}^2$ backing.

Johnson, Johnson, and Langer⁹ examined P^{32} , In^{114} , and Y^{90} in a high-resolution, 180° , shaped-magnetic-field spectrometer and reported the results in terms of a fit with a Fierz-interference-type shape factor $(1+b/w)$. The value for b ($0.2mc^2 < b < 0.4mc^2$) indicated an excess of about 15% at the low-energy side of the spectra for all three isotopes. A Na^{22} shape-factor plot¹⁰ obtained from the same instruments showed a decline of approximately 7% over the energy range from 50 keV to 450 keV, which is consistent with the same value for b as was obtained for the other three isotopes.

II. EQUIPMENT

An intermediate-image beta spectrometer^{11,12} was used for this investigation. The endplates had been modified to permit joint operation with a similar spectrometer for beta-beta coincidence measurements.¹³ Turns ratios in the coils were such that no shunted section was required to achieve intermediate-image focusing with the coils connected in series. A schematic diagram of the instrument is shown in Fig. 1.

The baffles were made of aluminum of $\frac{1}{2}$ -inch thickness. The baffle edges were angled approximately parallel to the central rays. Initially, data were taken without baffle B_1 in the spectrometer. P^{32} data were obtained with baffle settings giving 3.3% half-width and about 3% transmission. The baffle openings were

diminished to reduce the transmission by a factor of two resulting in a 2.5% resolution. No detectable change in shape factor occurred (see Table II). In^{114} data were taken with the baffles at the first-mentioned settings. Then B_1 was inserted with an opening, smaller than that which had been used for B_3 , which was then opened further to function mostly as a scatter baffle. A transmission of about $2\frac{1}{2}\%$ was obtained with a 2.4% half-width. No significant change in the In^{114} shape factor appeared at that time. Later, improved analytical methods gave a somewhat smaller slope for the shape factor in the latter set of data (see Table I), but the results are considered to be inconclusive for reasons that will be given later (Sec. IV).

To check for the possibility of distortion due to scatter off the edges of the openings at the ends of the spectrometer, endplates with polepieces¹² were reinstalled. No difference in the measured shapes of the In^{114} spectrum were detected.

Anthracene crystals, 2 mm thick, were used for beta detectors. A small diameter crystal, as it sublimates, would result in a changing transmission. A 1.0-cm orifice over a 1.4-cm diameter crystal was used for a constant detection area. The edges of the orifice were slanted at 45 degrees, meeting at a right angle in the central plane. The median angle for focussed electrons is about 45 degrees with respect to the spectrometer axis. The orifice was made in a $\frac{3}{8}$ -inch brass plate which is about twice the range of Y^{90} beta particles,¹⁴ the most energetic betas encountered in this research. The orifice also served to discriminate against any scattered electrons which approach the detector at angles greater than 45 degrees with respect to the spectrometer axis.

A 3-cm diameter crystal was tried as a detector. This

¹⁰ J. H. Hamilton, L. M. Langer, and W. G. Smith, *Phys. Rev.* **112**, 2010 (1958).

¹¹ H. Slatis and K. Siegbahn, *Arkiv. Fysik* **1**, 339 (1949).

¹² R. T. Nichols, A. V. Pohm, J. H. Talbot, Jr., and E. N. Jensen, *Rev. Sci. Instr.* **26**, 580 (1955).

¹³ H. Slatis and C. J. Herrlander, *Rev. Sci. Instr.* **26**, 613 (1955).

¹⁴ W. Paul and H. Steinwedel, in *Beta- and Gamma-Ray Spectroscopy*, edited by K. Siegbahn (Interscience Publishers, Inc., New York, 1955), p. 18.

was much larger than the area of focus so that sublimation could not affect the transmission. With this arrangement, the conversion lines in In^{114} had long tails on the low-energy side, and the shape-factor plots curved upward at the low-energy end. The results from both endplate arrangements varied with baffle openings, confirming the evidence that there was distortion due to detection of scattered electrons.

A 1.0-cm crystal was used with no orifice and corrections made for sublimation. No significant difference from the results with the 1.0-cm orifice was detected (see Table I).

Any orifice effects, whether from penetration or from scattering, would be enhanced with the replacement by a smaller orifice which places the orifice edges in a denser electron flux while diminishing the open area. A 0.6-cm orifice substantially changed the shape factor results, making the shape factors more positive and resulting in an approximately allowed shape for P^{32} . The absence of a measurable effect in changing from 1.0-cm orifice to the bare crystal indicates that the orifice effect was small in this case due to a relatively low number of electrons at the 1.0-cm periphery.

Sources were volatilized through a 5-mm orifice onto Formvar films. Some difficulty was experienced in obtaining substantial transfer of carrier-free activity to films of $50 \mu\text{g}/\text{cm}^2$ or less in thickness, without breaking the films. A rapid flash procedure was found to be the most efficient one. The thicknesses of films and sources were measured with an alpha gauge utilizing a ZnS scintillation detector and a Po^{210} alpha source. The discriminator level was set to eliminate the beta pulses for source thickness measurements. The sensitivity of the gauge was reduced when measuring high-energy beta sources, but a thickness of about $3 \mu\text{g}/\text{cm}^2$ could be detected.

An electron gun made from a 6AG5A tube was used to prevent source changing for much of the work. Later, a Po^{210} alpha source on a brass cylinder, $\frac{5}{16}$ inch in diameter, was covered with quarter-mil Al foil and placed 1 inch back of the beta sources to ground them.¹⁵

A 6810A 14-stage photomultiplier, cooled to -55°C , was used to amplify the beta signals. For the latter part

of this work an amplifier with gain settings from 20–100 was used with the results showing an improved signal to noise ratio. A univibrator with 15- to 20- μsec delay setting was employed to fix the dead time independent of energy and to eliminate counting of afterpulses.

As evidence for energy independence for the scintillation detection efficiency, plateau curves were obtained at various electron energies from 200 keV to 1430 keV by plotting the relative counting rate, after the thermal background had been subtracted, for a wide range of photomultiplier or amplifier gain settings. Such curves were taken frequently to check against changes that may appear with deterioration of optical junctions, phototube aging, etc. A pair of plateau curves at 200 keV and 900 keV are shown in Fig. 2. No need for detector efficiency corrections is evidenced for energies above 200 keV.

Current settings were maintained within about 2 ma by a servomechanism. An automatic current stepping device with data record was used to procure data in positive current steps over the desired energy range. Before going to a lower current setting, a homing cycle was used in which the current was increased to 100 amperes and then reduced to zero. This reduces variability from hysteresis. Current settings were found to repeat with a precision of better than 10 ma except for long-term drifts that are noticeable over a period of months. The actual current was measured frequently to give current values with errors less than one tenth of a percent. Calibration with $\text{Th}(B+C+C'')$ indicated linearity to 2.5 Mev within experimental error.

III. PROCEDURE AND TREATMENT OF DATA

Each set of data consisted of two or more runs over a spectrum. The data points were taken in order of increasing current settings starting from zero with the homing cycle taken before each run. Points below the detection threshold were used to obtain one background measurement and points beyond the spectrum for another. Beta sources made no noticeable contribution to the background.

A major portion of each spectrum was taken with the

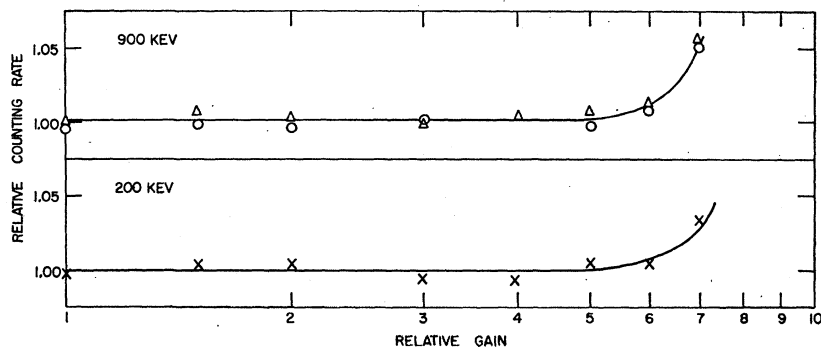


FIG. 2. Scintillation detection plateaus for two electron energies.

¹⁵ R. T. Nichols and E. N. Jensen, Rev. Sci. Instr. (to be published).

recorder operating for preset counts. In this mode of operation, counts on each data point are taken until the nearest tenth of a minute after the prescribed number of counts has been reached. Where the counting rate has dropped by a factor of five or more from the peak rate, a preset time interval was used on each data point so that an undue proportion of time was not spent in these regions.

Runs were programmed having total times of from 3 to 7 hours depending on the source strength. For the weaker sources (~ 5000 counts/min) many runs were used for a set of data to reduce uncertainties from possible background shifts during a run. Individual sets of data varied from 40 000 counts per data point to 90 000 counts per data point over the principal region.

An IBM-650 computer was used to calculate the results for all sets of data.

Half-life corrections never exceeded 4% in Y^{90} data and were much smaller for P^{32} and In^{114} . Comparison of corresponding points on successive runs over the spectrum indicated that the half-life corrections were sufficiently accurate for this work.

Maximum counting rates up to 20 000 counts/min resulted in dead time losses up to 0.5% for which compensation was made in the calculations.

Calibration accuracy was estimated to be about 0.1%. Since the maximum beta energy value which is used for a shape-factor plot was obtained from the same set of data, calibration errors could not affect the results significantly. A one percent change in calibration constant effects a change of $0.0006/mc^2$ in the slope of an In^{114} shape-factor plot.

The K -conversion lines from In^{114} were used to determine the spectrometer transmission functions. The 192-kev In^{114} conversion lines are shown in Fig. 3(a). The transmission function obtained from the K line is shown in Fig. 3(b). It has been obtained by plotting the K -electron counting rates versus ϵ , where

$$\epsilon = (I_p' - I')/I'$$

I' is the associated spectrometer current corrected for residual magnetism and I_p' is the corrected peak current value, i.e., the calibration reference point. The assumption was made that this function changes very little over the range of the spectrum as is the case if the shape of the magnetic field is constant and if scattering and penetration is negligible. The first and second moments of the normalized transmission functions were used to calculate the calibration constant change for a centroidal reference system and the resolution corrections¹⁶

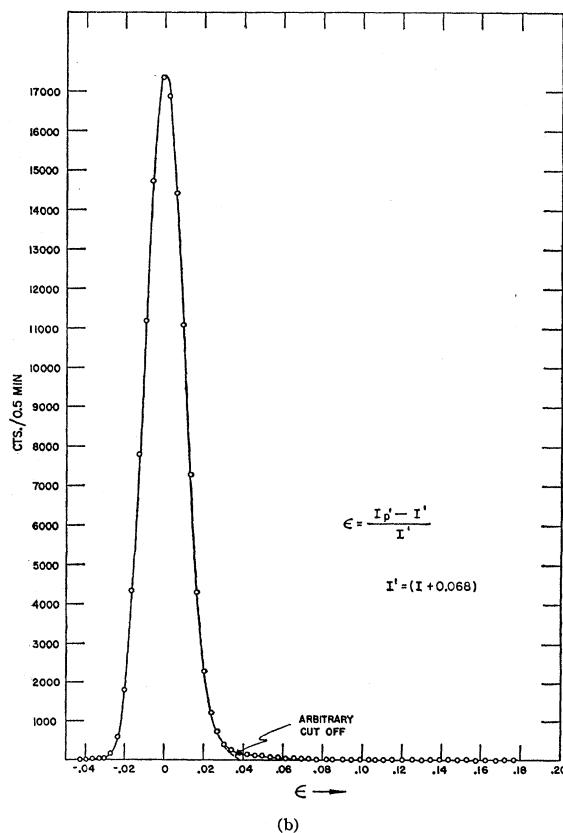
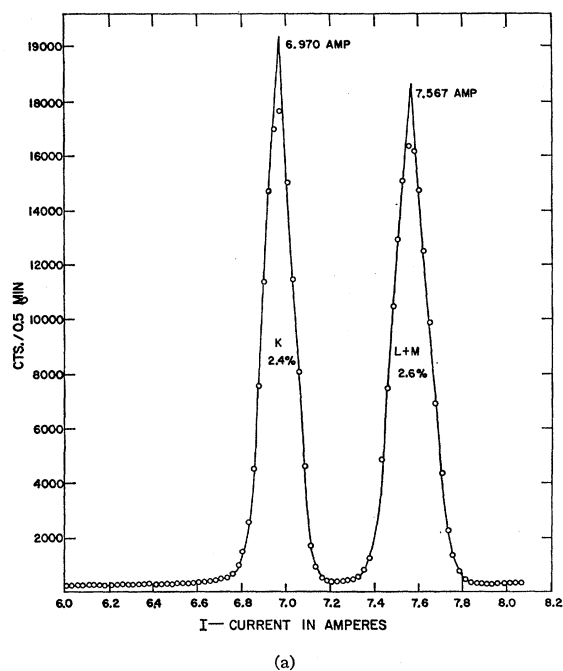


FIG. 3. (a) 192-kev conversion lines from In^{114} . (b) Spectrometer transmission function obtained from K -conversion line.

¹⁶ G. E. Owen and H. Primakoff, Phys. Rev. **74**, 1406 (1948); Rev. Sci. Instr. **21**, 447 (1950); F. T. Porter, M. S. Freedman, T. B. Novey, and F. Wagner, Jr., Phys. Rev. **103**, 921 (1956); Argonne National Laboratory Report ANL-5525 (unpublished).

which are minimal in this reference system. The theoretical beta distributions were taken as the true momentum distributions for the purpose of these calculations. No data point was used where the resolution correction exceeded 5%. The long tail on the upper side of the transmission line may be largely due to scattering which is expected to diminish at higher energies, or some of the tail may have been introduced by the use of a linear beta-background interpolation. The moments of the line were calculated using the arbitrary cutoff shown in Fig. 3(b) and again using the entire function. Median values were taken as the best estimates, and the limiting values were used to get indications of the uncertainties caused by the procedure. Over the energy range of the spectra in this study the effect of such errors in resolution corrections was not significant.

The quantities

$$y_i = N_i / (\eta_i^2 W_i r_i G_i S_i)$$

were calculated from the data. N_i is the counting rate with dead time, background and source decay corrections included, η_i and W_i are the associated momentum and energy in units of mc and mc^2 , respectively, r_i is the resolution correction, and G_i is the modified Fermi function

$$G_i = (\eta_i / W_i) F(Z, \eta_i)$$

obtained from tables¹⁷ with screening corrections added using interpolation from the tables of Reitz.¹⁸ S_i is an additional shape factor which contains the correction for finite de Broglie wavelength.¹⁹ For P^{32} and In^{114} it is the function L_0 and for Y^{90} it is the first forbidden unique shape factor, $9L_1 + (W_0 - W)^2 L_0$. The functions L_0 and L_1 were obtained from the tables of Rose *et al.*²⁰ The finite nuclear size has negligible effect on the shape of these spectra.^{21,22}

A quantitative measure of the deviation from theory was made in terms of a linear factor $(1 + aW_i)$, i.e.,

$$y_i = B(W_0 - W_i)^2(1 + aW_i) + \epsilon_i, \quad (1)$$

where B is a constant containing source strength and geometry factors, W_0 is the maximum beta energy, and ϵ_i is the statistical error. This three-parameter problem, with the unknown values of B , W_0 , and a , may be solved by a matrix method^{6,23} which requires initial estimates

¹⁷ M. E. Rose, N. M. Dismuke, C. L. Perry, and P. R. Bell, in *Beta- and Gamma-Ray Spectroscopy*, edited by K. Siegbahn (Interscience Publishers, Inc., New York, 1955), Appendix II, p. 875; Oak Ridge National Laboratory Report ORNL-1222, 1951 (unpublished).

¹⁸ J. R. Reitz, Phys. Rev. **77**, 10 (1950).

¹⁹ M. E. Rose and C. L. Perry, Phys. Rev. **90**, 479 (1953).

²⁰ M. E. Rose, C. L. Perry, and N. M. Dismuke, in *Beta- and Gamma-Ray Spectroscopy*, edited by K. Siegbahn (Interscience Publishers, Inc., New York, 1955), Appendix III, p. 884; Oak Ridge National Laboratory Report ORNL-1459, 1953 (unpublished).

²¹ M. E. Rose and D. K. Holmes, Phys. Rev. **83**, 190 (1951).

²² I. Malcom, Phil. Mag. **43**, 1011 (1952).

²³ O. Kempthorne, *The Design and Analysis of Experiments*, (John Wiley & Sons Inc., New York, 1952).

and through successive iteration will yield values arbitrarily close to the least-squares solution. Equations which are nonlinear in the unknown parameters may be linearized by a first order Taylor series expansion around approximate values for the parameters. The resulting equations are linear functions of correction parameters which may be solved for least-squares values. In the process, a matrix may be formed which contains estimates of the variances in the diagonal elements and estimates of covariances in the off-diagonal elements. The method is described in detail in reference 6.

The weighted sum of the residuals were treated in the form

$$\sum w_i \epsilon_i^2 = \sum n_i (y_i - A_i)^2 / A_i^2,$$

where

$$A_i = B(W_0 - W_i)^2(1 + aW_i),$$

and

$$n_i = (N_{Ti} - b t_i)^2 / (N_{Ti} + b t_i).$$

n_i is the relative weight or inverse square of the relative standard deviation assuming negligible variance from sources other than counting statistics. N_{Ti} is the total number of counts for the data point, b is the background in counts per unit time, and t_i is the counting time for the point. The substitution of A_i^2 for y_i^2 in the denominator of the residual expression simplifies calculations somewhat. The initial estimates for W_0 and B were computed from a weighted least squares linear fit of the allowed Kurie plot in the form

$$y_i^{1/2} = \alpha W_i + \beta + \delta_i,$$

where α and β are the unknown parameters and δ_i is the statistical error. The weights for this calculation are

$$w_i' = n_i / y_i.$$

Then, where $aW_0 \ll 1$,

$$W_0 \approx -\beta/\alpha \quad \text{and} \quad B \approx \alpha^2.$$

Starting with these approximate values of W_0 and B and the approximation of $a=0$, the three-parameter solution was obtained by use of successive iteration until the correction parameters were much smaller than the standard deviation values. The weighted sum of the residuals was then computed, as well as $y_i/B(W_0 - W_i)^2$, for the shape-factor plots using the resultant values for the three parameters.

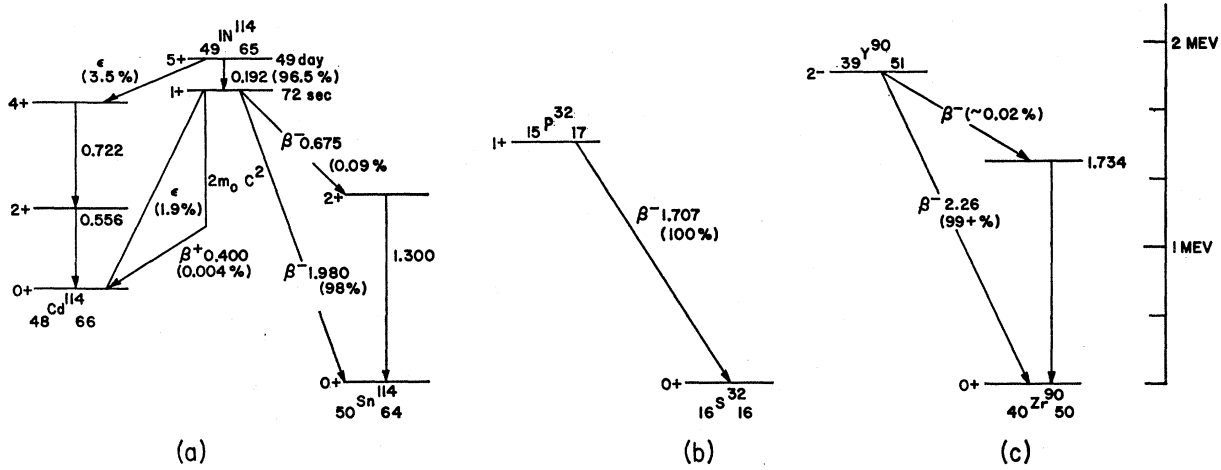
IV. RESULTS AND DISCUSSION

Indium-114

The accepted decay scheme^{24,25} of In^{114} is shown in Fig. 4(a). Beta systematics agree with shell model predictions that the ground state of an even-even nucleus is 0+ and that the first excited state is 2+

²⁴ J. N. Brazos and R. M. Steffen, Phys. Rev. **102**, 753 (1956).

²⁵ L. Grodzins and H. Motz, Phys. Rev. **102**, 761 (1956).

FIG. 4. (a) In^{114} decay scheme. (b) P^{32} decay scheme. (c) Y^{90} decay scheme.

except for special cases.²⁶ Therefore the ground state of In^{114} is $0+$ or $1+$ since it has allowed beta transitions ($\log ft$ values of 4.4 and 4.0) to both states in Sn^{114} . The K -conversion coefficient and the lifetime of the 192-keV transition from the isomeric level rule out the $0+$ assignment²⁷ since the angular momentum of the 50-day isomeric state has been measured to be 5.²⁸ Furthermore, K/L and $L_I:L_{II}:L_{III}$ ratios give an unambiguous $E4$ assignment²⁹ to the 192-keV transition. Thus the ground state beta transition must be a pure Gamow-Teller allowed transition.

Preliminary studies were made of In^{114} produced at Oak Ridge and at Brookhaven from neutron irradiation of indium. The sources were volatilized in the form of InCl_3 . Thick source effects appeared due to granulation caused by deliquescence and the subsequent loss of water in the spectrometer vacuum chamber. The source used for the final results was in the form of In_2O_3 . The In^{114} activity had been induced in In^{113} -enriched (60%) indium by neutron bombardment at Argonne National Laboratories. The source was volatilized onto a $45\text{-}\mu\text{g}/\text{cm}^2$ Formvar film. Alpha gauge measurements showed that the source was less than $3\text{ }\mu\text{g}/\text{cm}^2$ thick.

Table I shows the In^{114} results under differing conditions. Shape-factor plots from the same data are shown in Fig. 5. The Kurie plot is shown in Fig. 6, for the case of maximum deviation from the allowed shape. No points were taken at energies below 225 keV because of the conversion lines and the 0.7-MeV beta group. A small correction was adequate to compensate for the presence of the 0.7-MeV beta group in the region

studied. This correction was obtained from the relation

$$\frac{N_1(\eta)}{N_2(\eta)} = \frac{B_1 f_2 (W_{01} - W)^2}{B_2 f_1 (W_{02} - W)^2},$$

which holds when $\eta < \eta_{01}$, and $\eta < \eta_{02}$. $N_1(\eta)$ and $N_2(\eta)$ are the spectrometer counting rates for two beta groups from the same isotopes. B_1 and B_2 are the respective total activities; f_1 and f_2 are the associated integrals,

$$f = \int_0^{\eta_0} \eta W G(Z, \eta) d\eta,$$

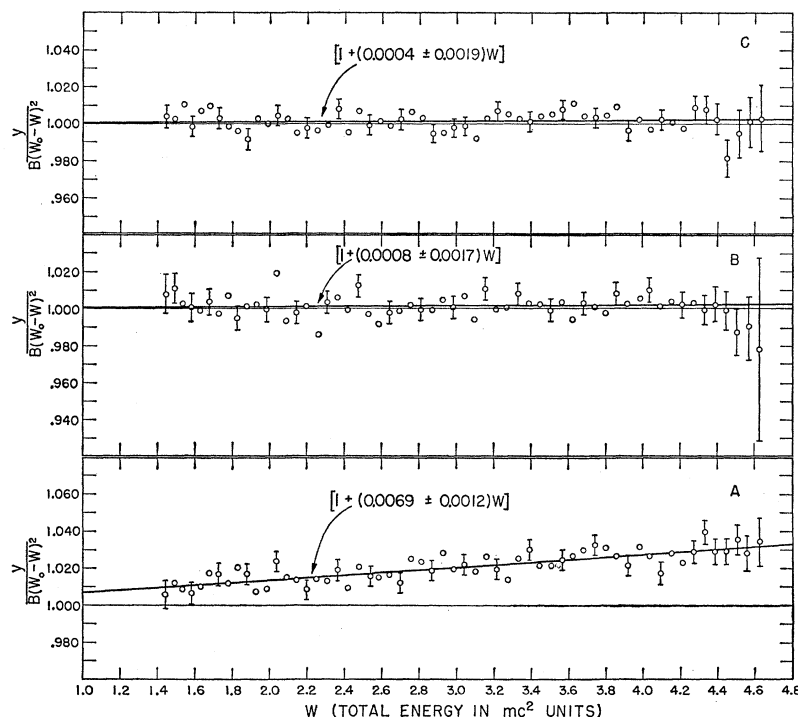
obtained from the graphs of Feenberg and Trigg³⁰; W_{01} and W_{02} are the maximum beta energies; and η_{01} and η_{02} are the maximum momenta. The shape factor plots show points with and without this correction. The result of the change is to increase the values for a by $0.0009/\text{mc}^2$.

The errors given in the tables and on the graphs are standard deviation estimates obtained from the least-squares calculations. From these results, it may appear that a definite change to closer agreement with theory occurs with the addition of the third baffle. However,

TABLE I. In^{114} results.

| Data set | Spectrometer variations ^a | a ($1/\text{mc}^2$) | W_0 (mc^2) |
|----------|---|-------------------------|-------------------------|
| A | B_2 and B_3 ; 1.0-cm orifice | 0.0078 ± 0.0012 | 4.8888 ± 0.0010 |
| B | B_1 , B_2 , and B_3 ; 1.0-cm orifice | 0.0017 ± 0.0017 | 4.8953 ± 0.0014 |
| C | B_1 , B_2 , and B_3 ; 1.0-cm crystal (no orifice) | 0.0013 ± 0.0019 | 4.8946 ± 0.0015 |

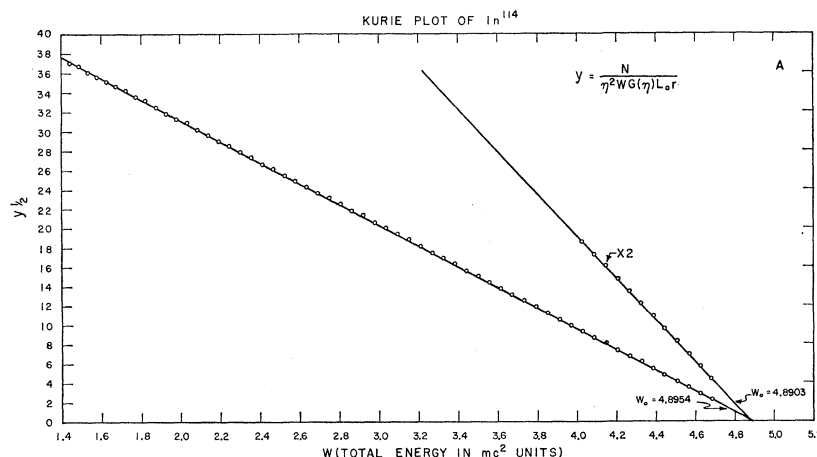
^a B_1 , B_2 , and B_3 are baffles (see Fig. 1).³⁰ E. Feenberg and G. Trigg, *Revs. Modern Phys.* **22**, 399 (1950).²⁶ G. Scharff-Goldhaber, *Phys. Rev.* **90**, 587 (1953).²⁷ R. M. Steffen, *Phys. Rev.* **83**, 166 (1951).²⁸ L. S. Goodman and S. Wexler, *Phys. Rev.* **100**, 1249(A) (1955).²⁹ V. M. Kelman, R. I. Metskhvarishvili, V. A. Romanov, L. I. Rusinov, and K. A. Konoplev, *Doklady Akad. Nauk. S.S.S.R.* **107**, 394 (1956) [translation: *Soviet Phys. (Doklady)* **1**, 189 (1956)].

FIG. 5. In^{114} shape-factor plots.

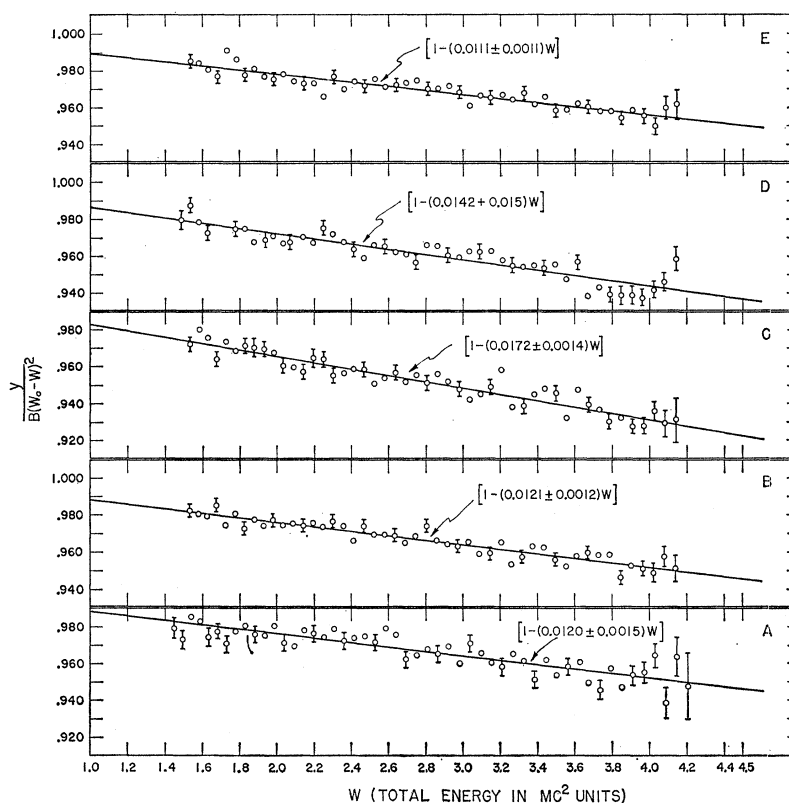
the values obtained for P^{32} (see Table II) indicated that such variations may occur with no apparent change in conditions. In view of this, the source of the additional variance is unknown. The number of measurements is too small for definite conclusions. An unweighted mean of the three measurements results in the value: $a = (0.0036 \pm 0.0021)/mc^2$. Errors quoted on the mean values in this paper are standard deviation estimates, in this case obtained from the deviations from the mean. Other factors are expected to contribute to the variance in W_0 . The unweighted mean of the W_0 values is $(4.8928 \pm 0.0013)mc^2$. When converted into Mev units, this becomes 1.989 ± 0.001 Mev. This agrees well with

the measurements of Johnson *et al.*⁹ obtained with volatilized sources and is slightly larger than those of Johns *et al.*³¹ obtained with a 1-mg/cm² source.

Five measurements of the 192-kev conversion peaks gave values of 162.7 ± 0.2 kev and 187.5 ± 0.2 kev for the K and $L+M$ conversion electron energies. A mean binding energy for the L electrons of 4.1 kev was obtained from the $L_I:L_{II}:L_{III}$ ratios of Kelman *et al.*²⁹ The affect of the M electrons on the location of the $L+M$ peak was estimated by construction of the composite line from the transmission function obtained from the K line using the L/M ratio given by Kelman *et al.* This gave a value of 3.8 ± 0.1 kev for the effective

FIG. 6. In^{114} Kurie plot from data set A.

³¹ M. W. Johns, C. D. Cox, R. T. Donnelly, and C. C. McMullen, Phys. Rev. **87**, 1134 (1952); Am. J. Phys. **31**, 225 (1953).

FIG. 7. P^{32} shape-factor plots.

binding energy of the $L+M$ electrons, from which a value of 191.3 ± 0.3 kev was obtained for the energy of the isomeric state. A value of 191.8 ± 0.2 kev was obtained from the K -line energy and the weighted mean of these two results is 191.6 ± 0.2 kev. This determination agrees well with the consensus of published results.³²

Phosphorus-32

The decay scheme of P^{32} is shown in Fig. 4(b). The spin of the ground state has been measured to be one.³³ This conforms to shell model prediction,³⁴ which leads to the conclusion that it is an allowed, I -forbidden Gamow-Teller transition.

Carrier-free P^{32} was obtained from Oak Ridge. Volatilized sources had no measurable thickness with the alpha gauge ($< 3 \mu\text{g}/\text{cm}^2$). The sources were on Formvar films from 40 – $50 \mu\text{g}/\text{cm}^2$ in thickness. $30 \mu\text{g}/\text{cm}^2$ of aluminum was volatilized onto the back side of one source for one set of measurements. The presence of P^{33} activity in the source material restricted the region of study to that above 250 kev.

The results from P^{32} are presented in Table II. The 1.0-cm orifice was used in the spectrometer for all these measurements. The changes made within the set of results are also shown in the table. The associated

shape-factor plots are shown in Fig. 7. The Kurie plots for the case of maximum deviation are shown in Fig. 8. A least-squares line through the points with the kinetic energy $E > \frac{3}{4}E_0$ gives a value for W_0 which, when used in a shape factor plot, results in a slope of $0.0149/\text{mc}^2$ compared to the $0.0172/\text{mc}^2$ from the three-parameter least-squares analysis. This change comes from a shift of only 1 kev in endpoint energy value.

The values for the slope fluctuate much more than is consistent with the standard deviation estimates obtained from the least squares evaluation. It occurs with no apparent change in experimental conditions. Further work is planned in hopes of clarifying these results. The

TABLE II. P^{32} results.

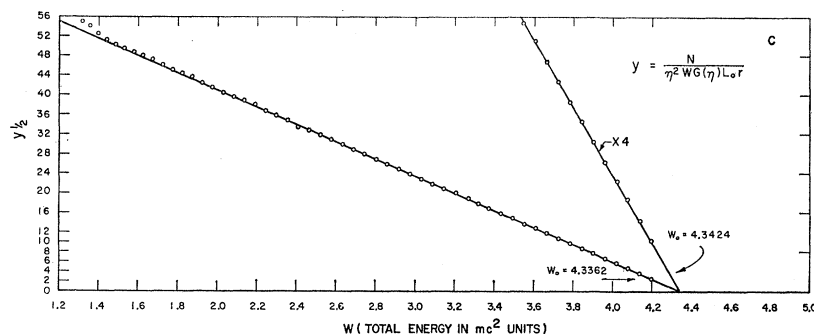
| Data set | Spectrometer variations ^a | a ($1/\text{mc}^2$) | W_0 (mc^2) |
|----------|--|-------------------------|-------------------------|
| A | B_2 and B_3 ; $1\frac{1}{2}\%$ T, 2.4% $W_{\frac{1}{2}}$ | -0.0120 ± 0.0015 | 4.3349 ± 0.0009 |
| B | B_2 and B_3 ; 3% T, 3.3% $W_{\frac{1}{2}}$ | -0.0121 ± 0.0012 | 4.3410 ± 0.0007 |
| C | B_1 , B_2 , and B_3 ; $2\frac{1}{2}\%$ T, 2.4% $W_{\frac{1}{2}}$ | -0.0172 ± 0.0014 | 4.3444 ± 0.0009 |
| D | B_1 , B_2 , and B_3 ; $2\frac{1}{2}\%$ T, 2.4% $W_{\frac{1}{2}}$ | -0.0142 ± 0.0015 | 4.3450 ± 0.0008 |
| E | B_1 , B_2 , and B_3 ; $2\frac{1}{2}\%$ T, 2.4% $W_{\frac{1}{2}}$ | -0.0111 ± 0.0011 | 4.3444 ± 0.0007 |

³² D. Strominger, J. M. Hollander, and G. T. Seaborg, Revs. Modern Phys. **31**, 585 (1958).

³³ G. Feher, Phys. Rev. **107**, 1463 (1957).

³⁴ L. H. Nordheim, Revs. Modern Phys. **23**, 322 (1951).

^a T—transmission; $W_{\frac{1}{2}}$ —half-width; B_1 , B_2 , and B_3 —baffles (see Fig. 1).

FIG. 8. P^{32} Kurie plot from data set C.

unweighted mean for the five sets of values yields

$$a = (-0.0133 \pm 0.0011)/mc^2$$

and

$$W_0 = (4.3419 \pm 0.0018)mc^2.$$

The latter value converted to Mev units is 1.7076 Mev. An average of 1.707 Mev has been computed from the results of thirteen investigations,³² most of which used Kurie plots from a major portion of the spectrum.

Henton and Carlson⁶ and Iben³⁵ have independently shown that for an l -forbidden transition a linear shape factor may be expected. Both used a tensor form for the Gamow-Teller interaction, but an axial vector interaction will give essentially the same results.³⁶ The theoretical calculations with simple shell-model wave functions predict a shape-factor slope of $-0.04/mc^2$,³⁶ which is appreciably larger than the result obtained in this investigation.

Yttrium-90

The accepted decay scheme for Y^{90} is shown in Fig. 4(c). The beta transition to the ground state of Zr^{90} must be once-forbidden, unique ($\Delta I=2$, yes) from nuclear shell model considerations,³⁴ the $\log ft$ value,³⁴ and the spectral shape.³⁷⁻⁴⁰

TABLE III. Y^{90} results.^a

| Data set No. | a ($1/mc^2$) | W_0 (mc^2) |
|--------------|----------------------|---------------------|
| A | -0.0052 ± 0.0016 | 5.4594 ± 0.0013 |
| B | -0.0044 ± 0.0013 | 5.4403 ± 0.0011 |
| C | -0.0034 ± 0.0016 | 5.4409 ± 0.0008 |
| D | -0.0038 ± 0.0026 | 5.4426 ± 0.0016 |
| E | -0.0080 ± 0.0022 | 5.4401 ± 0.0018 |

^a No variations in spectrometer arrangements.

³⁵ I. Iben, Jr., Phys. Rev. **109**, 2059 (1958).

³⁶ B. C. Carlson, in U. S. Atomic Commission Report ISC-1048 (Iowa State University) May, 1958 (unpublished).

³⁷ C. B. Broaden, L. Slack, and F. B. Schull, Phys. Rev. **75**, 1964 (1949).

³⁸ L. M. Langer and H. C. Price, Phys. Rev. **76**, 641 (1949).

³⁹ L. J. Laslett, E. N. Jensen, and A. Paskin, Phys. Rev. **75**, 412 (1950).

⁴⁰ J. Moreau and J. Perzy Jorba, Compt. rend. **235**, 38 (1952).

Carrier-free Y^{90} was obtained from Oak Ridge for this investigation. The sources were volatilized on 45–50 $\mu\text{g}/\text{cm}^2$ Formvar films. All measurements on Y^{90} were made with all three baffles in the spectrometer.

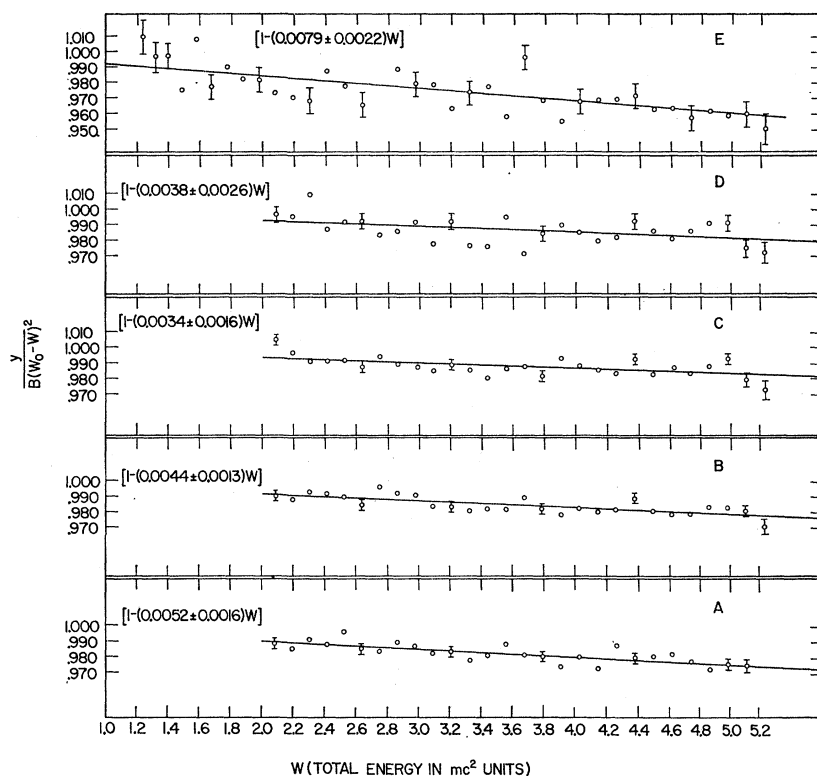
Table III presents the results from four sets of data for which the shape-factor plots are shown in Fig. 9. The fifth determination, which has the longer shape-factor plot, was made from a subtraction of the data for the D determination from the data for C determination which was taken one half-life earlier. This subtraction was used to eliminate Sr^{90} which may be considered to be a nondecaying component over this period of time. The other measurements were limited to the region beyond the range of the Sr^{90} spectrum which has a maximum energy at 550 kev. The results of the calculations for the In^{114} low-energy branch (see In^{114} discussion) indicate that no corrections are needed for presence of the 540-kev Y^{90} beta group from Y^{90} in the shape-factor plot E .

Since the five values obtained for a are not completely independent, the best estimation from these values is problematical. The unweighted and the weighted means using all values give identical results: $a = (-0.0047 \pm 0.0008)/mc^2$. The weighted sum of the squared residuals is 3.1. Thus the fluctuations are actually less than the expectation value in contrast to the results for In^{114} and P^{32} .

For W_0 the value obtained from the difference spectrum (E) was not used. The unweighted mean of the other values give $W_0 = (5.4453 \pm 0.0044)mc^2$ from which it may be determined that $E_0 = 2.271 \pm 0.002$ Mev. A value of 2.26 Mev has been computed from the results of eight investigations.³²

V. CONCLUSIONS

The beta spectrum of P^{32} has been measured and found to have a somewhat linear deviation from the allowed shape. The value for a , $(-0.0133 \pm 0.0011)/mc^2$, gives a magnitude of $3\frac{1}{2}\%$ for the total deviation over the energy range from 250 kev to 1600 kev. This is in good agreement with the results of Porter *et al.*,⁴ particularly since their method of analysis (in which a Kurie plot for $E > \frac{2}{3}E_0$ was used to obtain W_0) would give a slightly reduced shape-factor slope. It is much smaller

FIG. 9. Y^{90} shape-factor plots.

than has been predicted from theoretical considerations of l -forbiddenness.^{6,35,36}

Smaller deviations were obtained in the shape-factor plots of In^{114} : $a = (0.0036 \pm 0.0021)/mc^2$, and Y^{90} : $a = (-0.0047 \pm 0.0008)/mc^2$, with the In^{114} results not in definite disagreement with theory. Any instrumental distortions which may be conceived to account for the deviation in Y^{90} would be expected to affect the In^{114} results in the same direction, so we conclude that at least one of the two has a real deviation from the theoretical shape and, to a lesser degree of confidence,

that there is some deviation from theory in the spectrum of Y^{90} .

ACKNOWLEDGMENTS

The authors wish to express their appreciation to Dr. H. Daniel and Dr. B. C. Carlson for helpful discussions pertaining to this work. Gratitude is also expressed for the help of A. Booker in programming the IBM 650 for the treatment of data. Thanks also are due to K. Atkinson and K. Leonard for their assistance in calculations.